

# Influence of plasma spray parameters on mechanical properties of yttria stabilized zirconia coatings. II: Acoustic emission response

A. Kucuk, C.C. Berndt<sup>\*</sup>, U. Senturk<sup>1</sup>, R.S. Lima

*Department of Materials Science and Engineering, Center for Thermal Spray Research, State University of New York at Stony Brook,  
306 Old Engineering, Stony Brook, NY 11794-2275, USA*

Received 12 October 1999; received in revised form 7 February 2000

## Abstract

Yttria (8 wt.%) stabilized zirconia (YSZ) with a NiCrAlY bond coat was atmospherically plasma sprayed on mild steel substrates using various processing parameters including YSZ coating thickness, bond coat thickness, stand off distance, and substrate temperature. The cracking behavior of these coatings under four point bending load was examined using an acoustic emission (AE) recorder. The numbers of AE events exhibited during the elastic and plastic deformation of coatings were analyzed. Using multi-linear regression analysis, the number of AE events was correlated to the spray parameters. This analysis revealed that coatings with thicker YSZ top coat and NiCrAlY bond coat sprayed on a heated substrate at shorter stand off distance exhibited more AE activity and released higher AE energy under the bending. The greater emission activity and higher AE energy were evidence of severe cracking. © 2000 Elsevier Science S.A. All rights reserved.

*Keywords:* Thermal barrier coatings; Acoustic emission; Cracking behavior

## 1. Introduction

Plasma sprayed yttria stabilized zirconia (YSZ) coatings are used as insulative and corrosion resistant layers in high temperature applications such as gas turbine and diesel engines to enable higher working temperatures [1]. Plasma sprayed YSZ coatings, often referred to as thermal barrier coatings (TBCs), with their porous microstructure and ceramic nature provide good heat insulation to the main metal component. A NiCrAlY bond coat layer is applied to enhance adhesion strength between the metal component and YSZ coating. In addition, this NiCrAlY bond coat provides oxidation resistance to the main metal component at high temperatures [2].

Plasma sprayed YSZ coatings are built up from cohered splats that consist of a mixture of different phases. The characteristics of the coating depend pri-

marily on the feedstock powder, spray process parameters such as gun power, gas composition and flow rate, powder feeding rate, and equipment features such as gun type. As-received commercial YSZ feedstocks are generally mixtures of monoclinic and tetragonal phases [3], that may exhibit different size and shape distributions. Upon spraying, the majority of the powder melts and forms a metastable tetragonal phase ( $t'$ ) due to rapid solidification, while some of the particles stay un-melted and form a monoclinic phase [3]. These particles (splats) are randomly deposited and build up the coating. A coating can exhibit voids which are located between splats, due to random deposition and solidification, and within splats, due to solidification. In addition, processing stresses are generated in plasma sprayed coatings from rapid cooling and thermal expansion mismatch between the coating and substrate. These residual stresses vary throughout the thickness of the coating [4]. Some of the stresses are released by the formation of micro-cracks in ceramics [4,5], while residual stress, either compressive or tensile, is preserved in the coating. The type and the quantity of the residual stresses influence the coating performance. For example, it was reported that the adhesion and mechanical

<sup>\*</sup> Corresponding author. Tel.: +1-516-6328507; fax: +1-516-6328525.

E-mail address: cberndt@notes.cc.sunysb.edu (C.C. Berndt)

<sup>1</sup> Present address: PQ Corporation, Research & Development Center, 280 Cedar Grove Rd., Conshohocken, PA 19428-2240, USA.

Table 1  
Samples sprayed according to experimental design

Samples	Bond coat (µm)	Top coat (µm)	Substrate temperature (K)	Stand off distance (mm)
G1	100	300	393	80
G2	100	300	393	100
G3	250	300	393	80
G4	250	500	393	100
G5	250	500	393	80
G6	100	500	273	80
G7	100	500	273	100
G8	250	300	273	80
G9	100	500	393	80
G10	100	300	273	80
G11	250	300	393	100
G12	250	300	273	100
G13	250	500	273	80
G14	250	500	273	100
G15	100	300	273	100
G16	100	500	393	100
G17	175	400	333	

strength of the coatings directly related to the residual stresses [6]. Optimizing the spray parameters produces coatings with a desired microstructure (i.e. phase distribution, porosity, etc.) which determines coating performance. The deformation in YSZ coatings involves brittle fracture by crack initiation and growth as well as crack propagation from microcracks that evolve due to residual stresses. Therefore, it is crucial to understand cracking in ceramic coatings under load to characterize the deformation behavior of coatings. Cracks initiate and propagate during loading from defects such as pores, splat boundaries, secondary phase interfaces, and pre-existing cracks within coatings. A valuable tool in the analysis of cracks is to monitor acoustic emission (AE) response of deformation activities [7–10]. AE is a term describing a class of phenomena whereby transient elastic waves are generated by the rapid release of energy from localized sources within a material [11]. AE analysis has been successfully used to monitor cracking in ceramic coatings during mechanical testing (three point bending [12], four point bending [9,13], tensile adhesion test [14,15], and indentation [16]) and thermal cycling [8].

In the first part of this study [17], the influence of spray parameters such as top and bond coat thickness, stand off distance and substrate temperature on the mechanical properties of plasma sprayed YSZ coating were examined using a four point bend test. It was found that coatings with a thin bond coat sprayed on a cold substrate exhibited higher bending yield strength and bending modulus. However, stand off distance and top coat thickness were not found to have a statistically significant influence on the strength and stiffness of the coatings [17].

In the current work, the AE response of YSZ coatings under four point bend tests was investigated to further understand the cracking behavior of thermally sprayed YSZ coatings.

## 2. Experimental procedure

### 2.1. Sample preparation

Yttria (8 wt.%) stabilized zirconia (YSZ) was sprayed onto mild-carbon steel substrates under various process parameters including coating thickness (either 300 or 500 µm), stand off distance (either 80 or 100 mm) and substrate temperature (either at 273 or 393 K). In addition, the thickness of the atmospherically plasma sprayed bond coat, NiCrAlY, was varied as either 100 or 250 µm.

The substrates were grit blasted with alumina grit and cleaned with ethyl alcohol before spraying. The average roughness of the grit blasted substrate was  $4.0 \pm 0.5$  µm as measured with a Hommelwerke T1000 mechanical profilometer (Hommel America, New Britain, CT). Some of the substrates were pre-heated before spraying by using the plasma flame. The temperature of the substrates was measured using a hand held infrared temperature detector.

A statistical experimental design procedure using StatGraphics Plus 2.0 software (Statistical Graphics, Rockville, MD) was employed to determine the appropriate number of samples and spray parameters for relevant correlations. Table 1 gives the list of the samples sprayed in the current study according to this experimental design. Six samples from each group in Table 1 were sprayed with the conditions given in Table

2, using a Metco 3MB plasma gun (Sulzer-Metco, Westbury, NY). Further details of sample preparation have been presented elsewhere [17].

## 2.2. Four point bend test and in situ AE

The four point bend tests were performed using an Instron universal test machine (Model 8502, Instron, Canton, MA). The details of the four point bend test were previously given [17]. During the bend test, AE activities were monitored using an IBM compatible PC controlled MITRAS 2001 AE system (Physical Acoustics, Princeton, NJ). AE signals were received using a transducer of 22.5 mm diameter (model AC175L, Hartford Steam Boiler Inspection Technologies, Hartford, CT) placed on the steel substrate (in a non-coated location), and pre-amplified with a 2/4/6-AST model preamplifier (Physical Acoustics, Lawrenceville, NJ), and filtered with a 100H model preamplifier filter (Physical Acoustics). Details of AE data analysis were given elsewhere [18].

Six samples from each group were loaded under the four point bend conditions to generate results with a 95% confidence limit. To minimize artifacts from edge

cracking, the sides of the samples were polished with 600 mesh abrasive before the tests.

## 3. Results

### 3.1. Four point bend test

The bending yield stress and modulus, calculated from the load–displacement out put of the four point bend test, were reported previously [17]. The data are summarized in Table 3.

### 3.2. AE

Samples from each group exhibited different AE activity during four point bend tests (Fig. 1). Fig. 1 graphs the total AE events and sub-set of those generated only during the elastic regime. The activities were separated according to those generated during the elastic deformation and those generated after yield point. The influences of spray parameters on the numbers of AE activities in the elastic region are illustrated along with the total number of AE activities in Fig. 1. The trend in the number of AE response of the coatings sprayed with different parameters is similar in elastic and total deformation (Fig. 1). The order of groups according to the number of AE events in the elastic region and the total number, for example, is similar. Thus, the number of AE activities increases from  $G15 < G1 < G12 < G11 < G2 < G8 < G10$  to  $G3$  for the top coat thickness of 300  $\mu\text{m}$ . As seen in Fig. 1, five out of eight coatings revealed higher AE response under the four point test for increasing top and bond coat thickness while six out of eight coatings exhibited increasing AE activity for higher substrate temperature or shorter stand off distance. Further analysis of the effect of each spray parameter is given in Section 3.3.

Fig. 2 illustrates the comparison of total number of AE events with the number of AE activities in the elastic region. (The general trend is that samples with higher number of AE response in the elastic region, also exhibited higher total AE response). The samples in the groups can be separated into three categories according to AE response; i.e. high, medium, and low AE response. According to the number of AE events in the elastic region (i.e. the square boundaries in Fig. 2), groups 1, 12, 15, 16, and 17 are in the low response, and groups 2, 4, 6, 7, 8, 9, 10, 11, and 14 are in the medium response categories while groups 3, 5, and 13 are in the high response category. On the other hand, according to total number of AE activities (i.e. the ellipses in Fig. 2), the low response category includes groups 1, 11, 12, 15, and 16, while the medium response category consists of groups 2, 6, 7, 8, 10, 14, and 17, and the high response category includes groups 3, 4, 5,

Table 2  
Spraying parameters

	YSZ	NiCrAlY
Gun Type	Metco 3MB	Metco 3MB
Current (A)	600	500
Voltage (V)	70	70
Primary gas, Ar ( $\text{l min}^{-1}$ )	40	40
Secondary gas, H, ( $\text{l min}^{-1}$ )	11	8
Powder carrier gas, N, ( $\text{l min}^{-1}$ )	3.5	3.65

Table 3  
Summary of the mechanical properties of the coatings in this study [17]

Groups	Bending yield strength (MPa)	Bending modulus (GPa)
1	301 $\pm$ 23	114 $\pm$ 11
2	191 $\pm$ 52	72 $\pm$ 24
3	92 $\pm$ 38	29 $\pm$ 14
4	14 $\pm$ 18	4*4
5	225 $\pm$ 41	72 $\pm$ 17
6	160 $\pm$ 53	51 $\pm$ 19
7	260 $\pm$ 26	89 $\pm$ 11
8	328 $\pm$ 43	114 $\pm$ 7
9	62 $\pm$ 43	21 $\pm$ 14
10	206 $\pm$ 88	78 $\pm$ 36
11	27 $\pm$ 50	8 $\pm$ 14
12	73 $\pm$ 99	21 $\pm$ 29
13	250 $\pm$ 30	86 $\pm$ 15
14	1 $\pm$ 25	1 $\pm$ 6
15	440 $\pm$ 61	171 $\pm$ 17
16	371 $\pm$ 59	144 $\pm$ 19
17	11 $\pm$ 44	4 $\pm$ 13

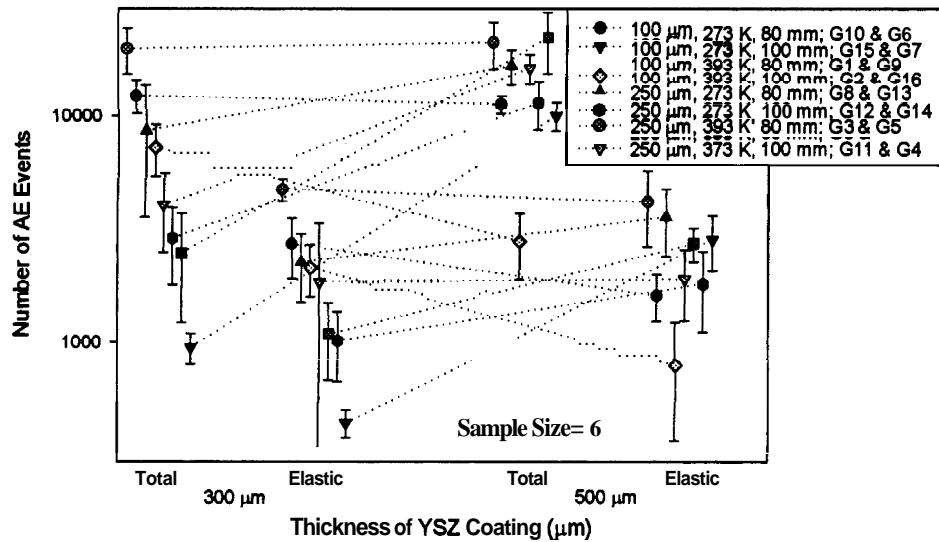


Fig. 1. Change in the numbers of acoustic emission (AE) activities under elastic and total deformation with spray parameters. The difference between the paired groups is the thickness of the yttria stabilized zirconia (YSZ) layer

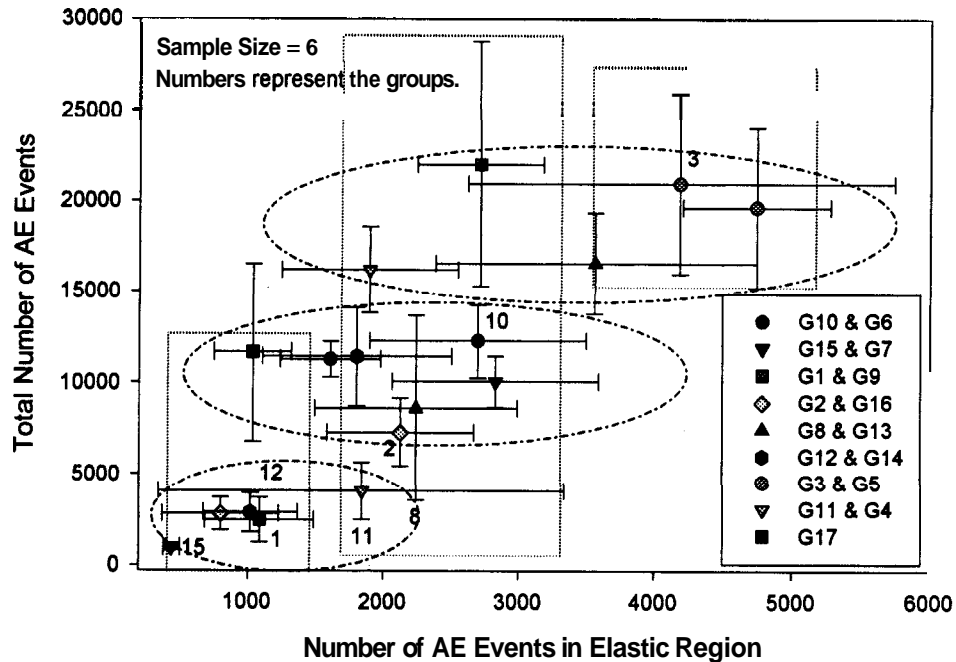


Fig. 2. Comparison of acoustic emission (AE) response of coatings under elastic and total deformation. Rectangles are for the categories according to AE response under elastic deformation while ellipsoids are for the categories according to acoustic response under total deformation.

9, and 13. There is no simple correlation between these categories and the spray parameters.

Since the energy of AE response is as important as the number of the AE response in understanding the deformation characteristic of coatings under load, the cumulative energy of the AE activities was calculated for each sample. Fig. 3 illustrates the change of cumulative energy with cross-head displacement in the four bend test. One should notice that only one representative curve out of six curves for each group is presented

in Fig. 3. The variation in cumulative energy of AE varied as high as 50% within a group. In Fig. 3 the cumulative energy value for AE activity in the elastic region is presented as an enlarged portion. As shown, a significant change in the cumulative energy of AE can be seen upon transition from an elastic to plastic deformation region. A similar change in the number of AE events was also observed upon the elastic–plastic deformation transition (Fig. 2). The same categorization proposed according to the number of AE events was

valid for the cumulative energy of AE activities (Fig. 3): Samples in groups 1, 2, 11, 12, 15, and 16 exhibited AE activities with low amounts of cumulative energy, samples in groups 6, 7, 8, 10, 13, 17 released medium amounts of cumulative energy, while samples in groups

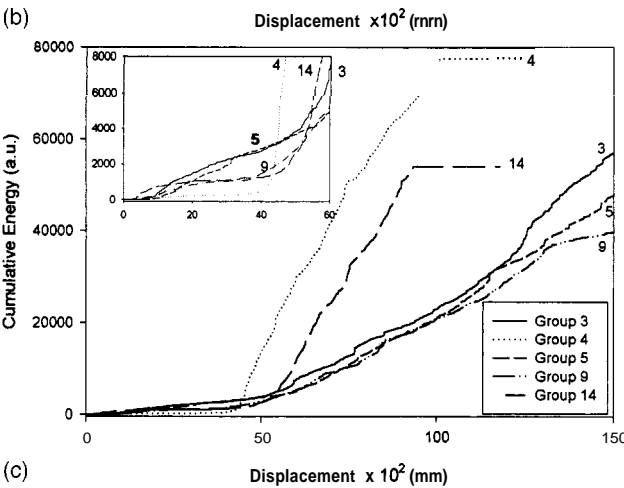
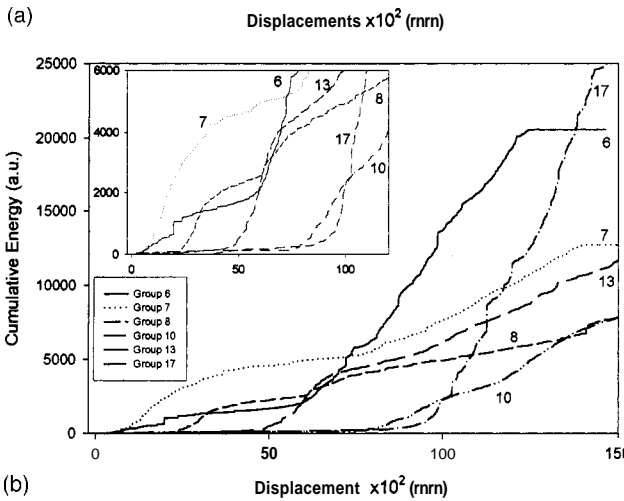
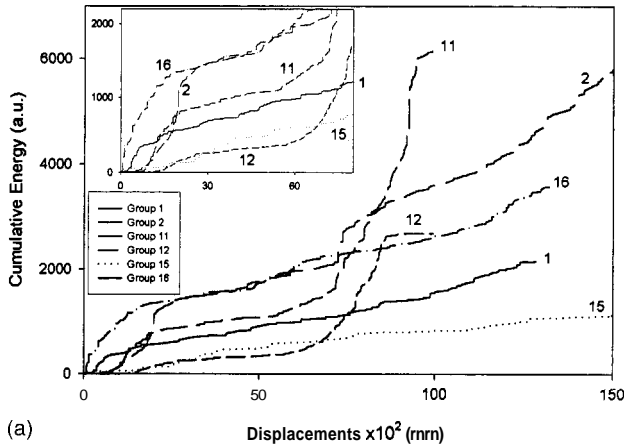


Fig. 3. (a) Change in cumulative acoustic emission (AE) energy of coatings with deformation. Inset illustrates the cumulative AE energy under elastic deformation. (b) Change in cumulative AE energy of coatings with deformation. Inset illustrates the cumulative AE energy under elastic deformation. (c) Change in cumulative AE energy of coatings with deformation. Inset illustrates the cumulative AE energy under elastic deformation.

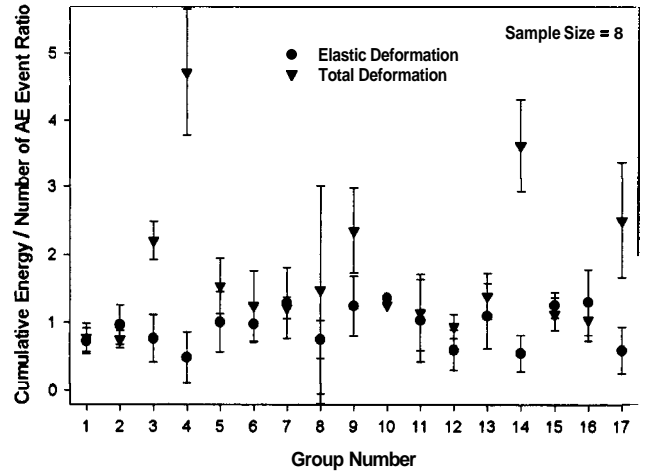


Fig. 4. Ratio of the cumulative acoustic emission (AE) energy to the number of AE events under elastic and total deformation.

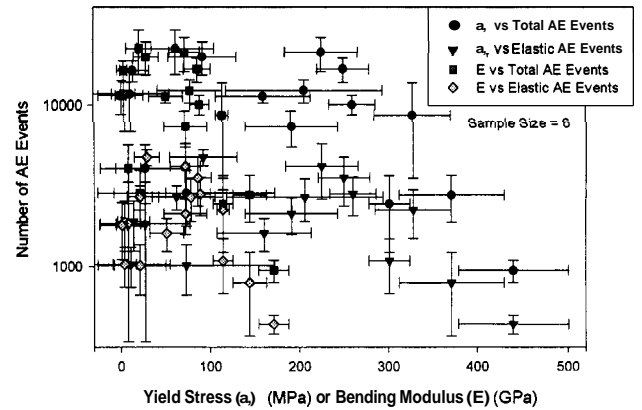


Fig. 5. Comparison of the number of acoustic emission (AE) activities with the mechanical properties of the coating measured in a previous study [17].

3, 4, 5, 9, 14 generated high amounts of AE cumulative energy.

The ratio of the cumulative energy to number of AE events for both elastic and total deformation is presented in Fig. 4. The ratios are similar except those for 3, 4, 9, 14, and 17.

In Fig. 5, the AE response of samples were compared with the mechanical properties of the coatings; bending yield strength and modulus measured in the previous study [17]. There is no simple correlation between the number of AE activities and the mechanical strength of the coatings.

### 3.3. Statistical analysis on results

To further understand the significance of each parameter on the AE response of the coatings, all the results were statistically analyzed using multi-linear regression.

Table 4  
Results of the multiple linear regression analysis on the spray parameter dependence of the number of acoustic emission (AE) activities during elastic and total deformation under four point bending of the coatings<sup>a</sup>

	Estimated coefficient		S.E.		t-test probability	
	Elastic	Total	Elastic	Total	Elastic	Total
Constant	4520.5	8291.6	1673.5	7224.3	0.007	0.255
$t_{BC}$ ( $\mu\text{m}$ )	5.9	28.2	1.7	7.7	0.001	0.001
$t_{TC}$ ( $\mu\text{m}$ )	2.2	39.0	1.3	5.8	0.094	0.000
$T_{St}$ (K)	4.1	25.9	2.2	9.7	0.065	0.009
$X_{sod}$ (mm)	-62.7	-303.4	13.0	57.7	0.000	0.000

<sup>a</sup>The t-test probability is the probability of each parameter not being statistically significantly influential. ( $t_{BC}$  is the thickness of bond coating (NiCrAlY) in  $\mu\text{m}$ ,  $t_{TC}$  is the thickness of the top coating (YSZ) in  $\mu\text{m}$ , and  $T_{St}$  is the substrate temperature in K,  $X_{sod}$  is the stand off distance in mm.)

Table 5  
The predicted changes in the number of the elastic and total acoustic emission (AE) response of the coatings during four point bend test<sup>a</sup>

	Change in parameter	Change in elastic AE response	Change in total AE response
$t_{BC}$ ( $\mu\text{m}$ )	+150	+888 $\pm$ 216	+4234 $\pm$ 1156
$t_{TC}$ ( $\mu\text{m}$ )	+200	+438 $\pm$ 256	+7791 $\pm$ 1156
$T_{St}$ (K)	+120	+487 $\pm$ 259	+3106 $\pm$ 1159
$X_{sod}$ (mm)	+20	-1254 $\pm$ 260	-6068 $\pm$ 1155

<sup>a</sup> Plus (+) and minus (-) signs indicate increase and decrease in the quantity, respectively. ( $t_{BC}$  is the thickness of bond coating (NiCrAlY) in  $\mu\text{m}$ ,  $t_{TC}$  is the thickness of the top coating (YSZ) in  $\mu\text{m}$ , and  $T_{St}$  is the substrate temperature in K,  $X_{sod}$  is the stand off distance in mm.)

### 3.3.1. Number of AE events in elastic region

A multi-linear regression analysis was applied to the results on the number of AE events monitored in the elastic region to examine the influence of the spray parameters using the Statgraphics Plus 2.0 software. An F-test validated the significance of a relationship between the four independent variables (bond coat thickness, top coat thickness, substrate temperature and stand off distance) and the number of AE activities in the elastic region at the 99% confidence interval. A Student t-test proved that bond coat thickness and stand off distance are significantly influential on the number of AE activities observed in the elastic region at the 99% confidence interval (Table 4) while top coat thickness and substrate temperature have significant influence on the number of AE activities at more than 90% confidence interval. The following equation from the fitted model relates the number of AE events in the elastic region,  $N_{AE}(\text{elastic})$  to the spray parameters in the studied interval:

$$N_{AE}(\text{elastic}) = 4520.6 + 5.92 \cdot t_{BC} + 2.19 \cdot t_{TC} + 4.06 \cdot T_{St} - 62.72 \cdot X_{sod} \quad (1)$$

where  $t_{BC}$  is the thickness of bond coating (NiCrAlY) in  $\mu\text{m}$ ,  $t_{TC}$  is the thickness of the top coating (YSZ) in  $\mu\text{m}$ ,  $T_{St}$  is the substrate temperature in K, and  $X_{sod}$  is the stand off distance in mm. The average value of residuals (mean absolute error) in the fit is 906.

While coatings with longer stand off distance exhibit smaller number of AE events, an increase in the bond or top coating thickness, and substrate temperature results in larger number of AE activities. An increase in bond coat thickness by 150  $\mu\text{m}$ , or in top coat thickness by 200  $\mu\text{m}$  causes 888  $\pm$  261 or 438  $\pm$  256 additional AE activities, respectively, while moving stand off distance from 80 to 100 mm results in a decrease in AE activities by 1254  $\pm$  260. The number of AE activities in the elastic region are higher by 487  $\pm$  259 for the coatings on pre-heated (393 K) substrates with respect to that on cold substrates (Table 5). As seen, the most influential parameter on the number of AE activities monitored in elastic region is the stand off distance. No such dependence could be detected from the classical bend test measurements.

### 3.3.2. Number of total AE events

A similar multi-linear regression analysis was applied on the total number of AE events to determine the effects of each spray parameter. An F-test shows that there is a statistically significance correlation between the four independent variables (bond coat thickness, top coat thickness, substrate temperature and stand off distance) and the total number of AE activities at the 99% confidence interval. The Student t-test proved that all the spray parameters are significantly influential on the total number of AE activities at the 99% confidence interval (Table 4). The dependence of the total number

of AE events on the spray parameters,  $N_{AE}(\text{total})$  can be expressed by the formula:

$$N_{AE}(\text{total}) = 8291.6 + 28.2 \cdot t_{BC} + 39.0 \cdot t_{TC} + 25.9 \cdot T_s - 303.4 \cdot X_{\text{sof}} \quad (2)$$

where  $t_{BC}$ ,  $t_{TC}$ ,  $T_s$ , and  $X_{\text{sof}}$  are as described above. The average value of residuals (mean absolute error) in the fit is 3750. It is clear from this analysis that a sample with thinner bond and top coat sprayed on a cold substrate at longer stand off distance releases a lower total number of AE activities under four point bending. A 150  $\mu\text{m}$  decrease in bond coat thickness lowers the total number AE events by  $4234 \pm 1156$  while a 200  $\mu\text{m}$  decrease in top coating thickness results in  $7791 \pm 1156$  drop in the total number of AE activities. Similarly, a 120° increase in the substrate temperature or a 20 mm decrease in the stand off distance causes  $3106 \pm 1159$ , or  $6068 \pm 1155$  increase in the total number of AE events, respectively (Table 5).

#### 4. Discussion

The analysis of the AE data requires correlation of the AE response of coatings under load with the microstructure. The plasma sprayed YSZ coating microstructure includes splats (lamellae), porosity, voids, microcracks, and un-melted particles [1]. Splats can be a mixture of different phases such as metastable tetragonal (t') and monoclinic [3]. Porosity can be inter-lamellar or within lamellar. Inter-lamellar pores mostly form from the random built-up of splats. In addition, the volume change during solidification results in pores between and within lamellae pores. Microcracks in the ceramic layer form from the processing stresses. Rapid solidification and mismatch between the thermal expansion coefficient of the substrate and coating are the sources of the processing stresses. Bianchi et al. [19] reported that tensile solidification stresses and compressive stresses from thermal expansion coefficient mismatch in YZS coatings yield tensile residual stresses. Greving et al. [20] found that residual stresses vary throughout the TBC with a 254  $\mu\text{m}$  YSZ top coat and a 76  $\mu\text{m}$  NiCrAlY bond coat layers on a Hastelloy Alloy X substrate: 30 MPa tensile stress on the surface of the top coating decreases to 10 MPa compressive stress in the middle of top coat, and then it increases back to 30 MPa tensile stress at the top coat bond coat interface. It reaches 60 MPa tensile stress in the bond coat, and drops to 5 MPa compressive stresses at the bond coat/substrate interface. The stresses in the substrate are 150 MPa compressive near the interface. Matejicek et al. [4] measured residual stresses in a 200  $\mu\text{m}$  NiCrAlY and a 200  $\mu\text{m}$  YSZ on a steel substrate as  $99 \pm 15$  MPa tensile and  $15 \pm 10$  tensile respectively using X-ray diffraction.

#### 4.1. Effect of stand off distance

As given in Eqs. (1) and (2), a change in stand off distance has the most significant influence on the number of AE events during the four point bend test. It has been reported that stand off distance does not influence the bending yield strength and modulus of plasma sprayed TBCs [17,21]. Ilavsky et al. [22] reported that percent porosity in plasma sprayed YSZ coating produced using plasma-spheroidized powders increases from 10 to 14 vol.% with a change in the spray distance from 65 to 145 mm; while the crack surface area decreases by half with the same change in the spray distance. The decrease in the crack surface area implies that the residual stresses in a YSZ coating decreases with increasing spray distance. When temperature and particle velocity in the plasma plume are taken into consideration, it is reasonable to have higher stresses for shorter spray distances. Both the temperature and velocity of particles decreases with increasing distance from the plasma source. For example, the temperature and velocity of the particles in the plasma flame may vary as much as 1000 K, and 100  $\text{m s}^{-1}$  in a 20 mm change in the stand off distance. Higher particle temperatures result in a higher amount of quenching (solidification) residual stresses. In addition, the density and viscosity of particles are lower for higher temperatures. Therefore, particles spread better according to the Madejski equation [1]. Higher particle temperatures also provide more effective packing of splats, and better cohesion between splats. The decrease in percentage porosity and roughness, and increase in hardness is an indication of this more effective packing and cohesion between splats. Therefore, one would think that a coating with more effective packing and better cohesion would exhibit a lower AE response under load, i.e. coatings sprayed at lower spray distance would be expected to exhibit less AE activity. However, the converse is experimentally observed whereby an increase in spray distance decreases the number of AE activities recorded during a four point bend test. This arises because one should also consider changes in residual stresses with stand off distance because any tensile residual stresses present in the coating will be relieved by crack formation. For example, a 10 MPa tensile residual stress can be relieved by formation of 0.1  $\text{m}^2 \text{m}^{-3}$  fracture surface; i.e. crack formation. The crack surface was calculated by taking the fracture surface energy of YSZ as 50  $\text{J m}^{-2}$  [23]. Wigren et al. [24] reported that when spray distance change from 'short' to 'long' in spraying of a 420  $\mu\text{m}$  YSZ, residual stresses measured by the modified layer-removal method dropped by 40–50%. The decrease in AE activity ob-

<sup>1</sup>The exact spray distance in the mentioned study was not given, but just referred as 'short' and 'long'.

served by increasing spray distance implies that the effect of residual stresses on AE response of the coatings are the more dominant of effects from two parameters; residual stresses, and packing and cohesion efficiency.

The influence of processing stresses on AE response of coatings are 2-fold: (i) higher amount of processing stresses generate higher amount of microcracks which weaken the mechanical strength of coatings; and (ii) higher residual stresses from greater processing stresses promote cracking during loading. The microcracks formed during the release of processing stresses propagate under the load and generate AE energy. Therefore, AE analysis is a powerful tool to characterize the influences of processing and residual stresses. As given in Eqs. (1) and (2), the coefficient for stand off distance, estimated from multi-linear regression analysis, is high with respect to other parameters. The effect of stand off distance on the number of AE activities is more pronounced in the elastic region than the total deformation. It is believed that the more pronounced effect of stand off distance on the AE activities can be related to residual stresses. The load applied during the four point bend test promotes the relief of residual stresses by cracking. One should note that residual stress can not cause cracking unless they overcome the threshold value which is the minimum energy required to create a fracture surface. Lin et al. [25] carried out four point bend tests with varying loads on a YSZ TBC which yielded at a 3000 N bending load. They monitored AE response of a coating during the four point bend test under subsequent loads. They found that the number of AE activities changes as 460, 436, 186, 203, and 42 525 under the applied loads of 250, 1000, 1500, 2500, and 4800 N, respectively. As seen, the majority of the AE energy in the elastic region was released during the initial two loadings. This can be interpreted as an evidence for the relief of residual stresses by cracking during the first two loadings. Therefore, the more pronounced effect of stand off distance, which is driven by the amount of stresses, on the AE activity in the elastic region is reasonable.

#### 4.2. Effect of top coat thickness

As given in Eqs. (1) and (2), coatings with a thicker YSZ top coat generate more AE events in the four point bend test. One obvious reason for such AE response is the size effect. Since the volume of the thicker top coating is greater than that of a thinner coating, the number of cracks present after the spray process and generated during loading is higher for a larger volume. However, an increase in the AE activity with increasing top coat thickness can not be rationalized only by the size effect because otherwise the coefficients (2.18 and 38.96) for elastic and total deformation

would have been the same. In addition to a slight contribution from the size effect, the change in residual stresses due to thickness plays a significant role in the AE response of coatings. It was reported that residual stresses increased with the coating thickness [4].

The contribution of the top coat thickness with respect to the AE response of coating drastically increases after the yield point. As seen in Eqs. (1) and (2), the top coat thickness coefficient jumps from 2.19 to 38.89 for elastic and total deformation, respectively. Part of the reason for this observation is the nature of the test. In the four point bend test, the arrangement is such that the coating is under tension. The bending strain increases with respect to the distance from the neutral axis, and it is the highest on the outer layer of the coating. Therefore, the top coat undergoes the greatest amount of deformation, and the difference in the strain of the layer gets larger upon an increase in cross-head displacement during the four point bend test. As a result, a large contribution is observed with regard to the influence of top coat thickness on AE activity after the yield point. One other reason for a large change in the number of AE events after the yield point could be the delamination. After a certain amount of deformation, layers separate because of shear forces originating from the bending load. The AE energy emitted from such events (delamination) is much higher than the energy rising from vertical cracks. As given in Fig. 4 the cumulative energy increases after the yield point.

#### 4.3. Effect of bond coat thickness

The number of AE events increases with increasing bond coat thickness for both elastic and total deformation as given in Eqs. (1) and (2). Similar to the rational for the influence of top coat on the AE response, residual stresses play a significant role. One should notice that the residual stresses are much higher in the metallic bond coat than in the ceramic top coat since the bond coat is ductile with respect to brittle ceramic coating; i.e. residual stresses in the ceramic can be relieved by cracking processes. The effect of bond coat thickness on AE activity is more pronounced in the elastic and this might indicate relief of residual stresses upon initial loading.

#### 4.4. Effect of substrate temperature

Coatings sprayed on a pre-heated substrate exhibited more AE events as given in Eqs. (1) and (2). It has been reported that higher substrate temperature generally lowers the residual stresses in the coating layers [5]. Therefore, one would expect that coating on a pre-heated substrate should have given a lower number of AE activities. However, one should also consider other contributions such as oxidation and surface roughness.

Even though the temperature of the pre-heated substrate is reported as 393 K in the current study, it is believed that the local temperatures could be far more than the measured values. These local high temperature areas in the steel substrate give rise to oxidation of the substrate that lowers adhesion between the substrate and the bond coat. In addition, it also affects the deposition built-up such a way that packing could change.

#### 4.5. Energy of events

Although it is difficult to directly correlate the nature of cracking and the AE energy, it was attempted to determine the average energy per cracking. The ratio of cumulative energy to the number of AE events is given in Fig. 4. One is cautioned that rather than an average energy per cracking, a distribution of energy and cracking is more close to reality. Nevertheless, it is believed that the ratios represented in Fig. 4 present useful information. Strikingly, the ratios for elastic and total deformation and for different coating are of the same magnitude within the errors except coatings from groups 3, 4, 9, 14, and 17. At this point, no clear understanding on this observation was developed.

### 5. Conclusions

The cracking behavior of plasma sprayed TBCs under a four point bend loading was monitored using an in situ AE analysis. Depending on the spray parameters, the coatings exhibited different AE responses that were characteristic different amounts of AE energy. AE response of the coating during elastic and plastic deformation were differentiated, and analyzed separately. The number of AE events and AE energy released increased significantly after the yield point. However, the ratio of cumulative AE energy to the number of AE events under elastic and plastic deformation was similar for the coatings sprayed using different spray parameters except for coatings from groups 3, 4, 9, 14, and 17. For those exceptional groups, the ratio under total deformation was much higher than the ratio under elastic deformation.

A multi-linear regression analysis, applied on the AE activity monitored during elastic and plastic deformation of coatings, revealed that coatings with thinner bond and top coats sprayed on cold substrate at longer stand off distance exhibited a lower degree of cracking. The stand off distance within these four parameters was the most influential parameter on the AE response of coatings. It is believed that cracking behavior of coatings under four point bend loading is strongly controlled by the stresses created during processing due to rapid cooling and thermal expansion mismatch between

the coating layers and the substrate. Some of the processing stresses release by cracking in the coating. These cracks behave as sites for further cracking and crack propagation during loading. In addition, the tensile residual stresses in the coating promote cracking during loading.

The bending yield strength and modulus of coatings calculated in a previous work [17] was compared with the AE response of coatings. At the current stage of the work, no simple correlation between the bending strength and the AE response of coatings has been developed, however, further studies are being carried out.

### Acknowledgements

The authors would like to thank Dr Carlos R.C. Lima of University of Piracicaba, Brazil for his help with sample preparation during his sabbatical stay in SUNY at Stony Brook. This work was sponsored under NSF-MRSEC DMR grant number 9632570.

### References

- [1] L. Pawlowski, *The Science and Engineering of Thermal Spray Coating*, Wiley, New York, 1995.
- [2] R.A. Miller, *Surf. Coat. Technol.* 30 (1986) 1–11.
- [3] R.S. Lima, U. Senturk, C.C. Berndt, C.R.C. Lima, in: E. Lugscheider, P.A. Kammer (Eds.), *United Thermal Spray Conference*, German Welding Society, Dusseldorf, Germany, 1999, pp. 190–195.
- [4] J. Matejicek, S. Sampath, J. Dubsy, *J. Thermal Spray Technol.* 7 (1998) 489–496.
- [5] M. Levit, I. Grimberg, B.Z. Weiss, *Mater. Sci. Eng. A206* (1996) 30–38.
- [6] D.J. Greving, J.R. Shadley, E.F. Rybicki, *J. Thermal Spray Technol.* 3 (1994) 371–378.
- [7] C.C. Berndt, *J. Eng. Gas. Turbines Power-Trans. ASME* 107 (1985) 142–146.
- [8] J. Voyer, F. Gitzhofer, M.I. Boulos, *J. Thermal Spray Technol.* 7 (1998) 181–190.
- [9] U. Senturk, R.S. Lima, C.C. Berndt, C.K. Lin, C.R.C. Lima, in: E. Lugscheider, P.A. Kammer (Eds.), *United Thermal Spray Conference*, German Welding Society, Dusseldorf, Germany, 1999, pp. 815–819.
- [10] C.K. Lin, C.C. Berndt, *Surf. Coat. Technol.* 102 (1998) 1–7.
- [11] M.J. Noone, R.L. Mehan, in: R.C. Bradt, D.P.H. Hasselman, F.F. Lange (Eds.), *Fracture Mechanics of Ceramics*, Plenum Press, New York, 1974, pp. 201–229.
- [12] C.C. Berndt, D. Robins, R. Zatorski, H. Herman, Presented at 10th International Thermal Spraying Conference, Essen, Germany, 1983.
- [13] C.K. Lin, C.C. Berndt, S.H. Leigh, K. Murakami, *J. Am. Ceram. Soc.* 80 (1997) 2382–2394.
- [14] C.C. Berndt, *Mech. Eng.* 106 (1984) 85–85.
- [15] C.C. Berndt, *Mater. Sci. Forum* 34–36 (1988) 457–461.
- [16] S. Safai, H. Herman, K. Ono, Presented at 9th International Thermal Spraying Conference, Hague, Netherlands, 1980.
- [17] A. Kucuk, C.C. Berndt, U. Senturk, R.S. Lima, C.R.C. Lima, *Mater. Sci. Eng. A* 284 (2000) 29–40.

- [18] C.K. Lin, S.H. Leigh, C.C. Berndt, *Thin Solid Films* 310 (1997) 108–114.
- [19] L. Bianchi, F. Blein, N. Baradel, in: C.C. Berndt (Ed.), *Thermal Spray: A United Forum for Scientific and Technological Advances*, ASM International, Materials Park, OH, 1997, pp. 831–838.
- [20] D.J. Greving, E.F. Rybicki, J.R. Shadley, *J. Thermal Spray Technol.* 3 (1994) 379–388.
- [21] P. Boch, P. Fauchais, D. Lombard, B. Rogeaux, M. Vardelle, in: N. Claussen, M. Rühle, A.H. Heuer (Eds.), *Advances in Ceramics Science and Technology of Zirconia II*, vol. 12, American Ceramic Society, Columbus, OH, 1984, pp. 488–502.
- [22] J. Ilavky, G.G. Long, A.J. Alen, H. Herman, C.C. Berndt, in: C.C. Berndt (Ed.), *9th National Thermal Spray Conference*, ASM International, Materials Park, OH, 1996, pp. 725–728.
- [23] W.D. Kingery, H.K. Bowen, D.R. Uhlmann, *Introduction to Ceramics*, 2nd edition, Wiley, New York, 1976.
- [24] J. Wigren, L. Pejryd, B. Gudmundsson, R.T.R. McGrann, D.J. Greving, E.F. Rybicki, J.R. Shadley, in: C.C. Berndt (Ed.), *9th National Thermal Spray Conference*, ASM International, Materials Park, OH, 1996, pp. 847–854.
- [25] C.K. Lin, U. Senturk, R.S. Lima, C.C. Berndt, J.C. Shieh, P.Y. Lee, in: E. Lugscheider, P.A. Kammer (Eds.), *United Thermal Spray Conference*, German Welding Society, Dusseldorf, Germany, 1999, pp. 809–814.